J. Phys. F: Met. Phys., **12**(1982)2499–507. Printed in Great Britain

The solid–liquid transition in mercury based magnetic fluids

S R Hoon‡, J Popplewell† and S W Charles†
† School of Physical and Molecular Sciences, University College of North Wales, Bangor, Gwynedd, LL52 2UW, Wales, UK
‡ Department of Physics, University of Durham, South Road, Durham DH1 3LE, England, UK

Received 24 August 1981, in final form 27 May 1982

Abstract. The solid–liquid transition for magnetic fluids containing iron particles in mercury and iron particles in tin–mercury has been investigated using a differential scanning calorimeter. The detail of the phase change near the melting point has been found to be dependent upon both the iron particle concentration and, when present, the spatial location of tin metal additives. The measurements are interpreted in terms of particle interactions.

1. Introduction

Magnetic fluids consist of single domain magnetic particles dispersed within a carrier liquid. Non-metallic based fluids, such as the ferrite–diester ferrofluids manufactured by Ferrofluidics Corporation (Nashua, NH, USA), are used as sealants in high-speed rotary vacuum seals and as damping and supporting fluids in stepper motor dampers and loudspeaker voice coil assemblies. Metallic based magnetic fluids, that is fluids which utilise a liquid metal as the carrier liquid, are not as highly developed nor available commercially. However the possible use of metallic based fluids for brushless commutators and ferromagnetohydrodynamic energy conversion devices has stimulated much recent research (Charles and Popplewell 1978, 1980), in particular into the properties of mercury based fluids. If a magnetic fluid is to be used in devices it must be stable over the lifetime of the device and aggregation of the colloidal ferromagnetic particles must be prevented. Such stability may only be achieved by ensuring that the attractive particle interaction energy, due to the van der Waal and magnetic dipole forces, never exceeds the Boltzmann energy kT. In practice this condition is obtained by making the particles small and by introducing a particle–particle repulsive interaction. In non-metallic based fluids, particle repulsion is achieved via the entropic repulsion of a particle surfactant, such as oleic acid (Rosensweig *et al* 1965). Mercury based fluids, however, cannot be stabilised by the surfactants used in non-metallic carrier systems and alternative methods of producing repulsive forces between particles have to be considered. Charge layer repulsion between particles in metallic based fluids has been suggested as a possible stabilising force (Popplewell *et al* 1976). However recent calculations (Hoon 1980) based upon a model of the bimetallic junction due to Bennett and Duke (1967a, b) imply that the extent of the charge layer at an

0305-4608/82/112499 + 09$02.00

iron–mercury interface may be too small to overcome the attractive interparticle forces present in these fluids. The calculations, however, are not exact and there is a need for a more complete theory to describe short-range forces between particles in metallic systems.

It has been found by Luborsky (1957, 1962a, b) and Windle *et al* (1975) that, in the absence of any additives, iron particles grow in liquid mercury by interparticle diffusion of iron atoms. The iron atoms diffuse from the high-energy surfaces of small particles to the low-energy surfaces of large particles. The particle growth rate is found to accelerate when the temperature of the fluid is increased. The growth rate, which has been found by Windle *et al* (1975) to be approximately described by the equation of Greenwood (1956) is determined by several factors. These include the particle size distribution, the small but finite solubility of iron in mercury (less than 10^{-5} wt% at 300 K, Bailar 1973) and the presence and coalescence of particle aggregates. However a significant reduction in the particle growth rate has been achieved by the addition of elements such as tin, antimony and sodium (Falk and Luborsky 1965, Windle *et al* 1975, Popplewell *et al* 1976, Dixon *et al* 1981), although their inclusion alone is insufficient to completely prevent particle aggregation. In this paper a study of the change in state from solid to liquid for iron–mercury fluids is reported. The results of this study support the conclusions made by Windle *et al* (1975) and Popplewell *et al* (1976) that particle growth, resulting from the diffusion of iron atoms, is inhibited by the tin additives forming particle coatings.

2. Experimental procedure

Fluid samples were prepared by the electrodeposition of iron from a saturated solution of ferrous chloride onto a strongly agitated cathode of triply distilled mercury. The cathode current density and cell temperature were kept constant at 60 mA cm^{-2} and 288 K respectively. The iron concentration of the fluids was determined from their saturation magnetisation. The median iron particle size, and any subsequent particle growth was inferred from measurements of the coercivity of frozen samples of the fluids at 77 K (Luborsky 1962a, b). No changes in the median particle size were detected during the course of the experiments. Tin additives were made by dissolving high-purity metal directly into the iron–mercury fluid. It was usual to add sufficient tin to form a monolayer coating on the iron particles. In calculating the amount of tin that was necessary to form a monolayer coating it was assumed that the tin atoms are hexagonally close-packed on the iron particle surface (Luborsky 1962a, b). It then follows directly that the total quantity of tin absorbed is given by

$$m_2 = m_1 \sqrt{3} A_2^{1/3} (2\rho_2)^{2/3} (N^{1/3} \rho_1 r)^{-1} \tag{1}$$

where m_1 denotes the total mass of the particles of median radius r and density ρ. N, A_2 and ρ_2 refer to Avogadro's number and the atomic weight and density of tin respectively.

Thermal analysis of the fluids was carried out using a commercial Perkin Elmer differential scanning calorimeter (DSC). The output of the DSC is derived from the differing quantities of heat required per unit time to raise the temperature of an encapsulated sample of fluid and an identical empty reference encapsulation can through equal temperature intervals.

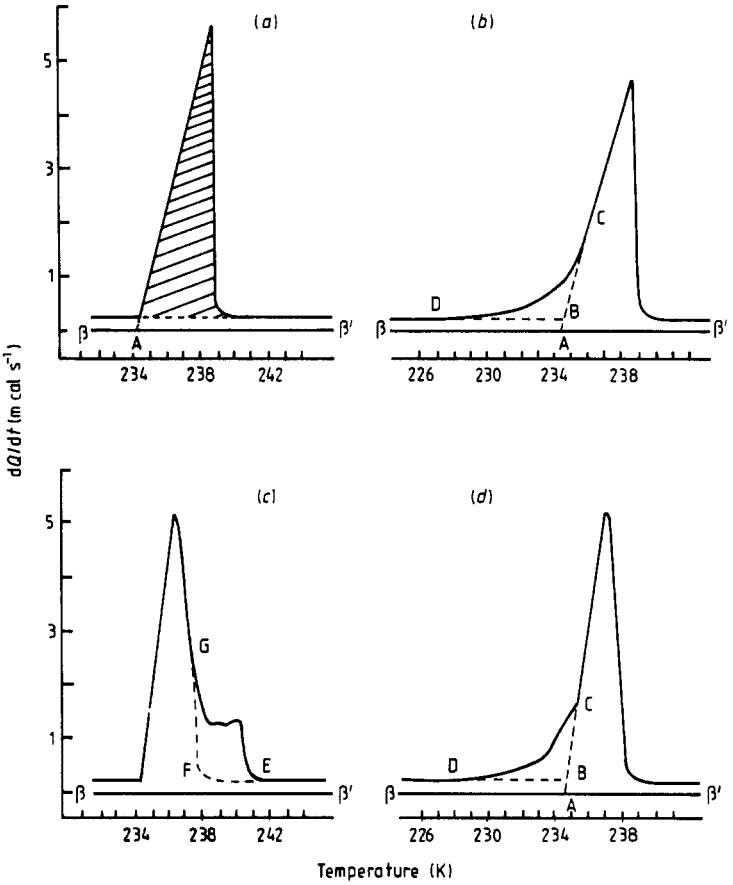

Figure 1. The DSC melting line shapes at scan rates of 3 K min^{-1} for (*a*) 99.999% pure mercury: the shaded area represents the latent heat transition, (*b*) 0.75 wt% Fe particles in Hg fluid: the broken line indicates the bulk melting edge, (*c*) 0.4 wt% Sn in Hg liquid alloy, (*d*) 0.4 wt% Sn + 0.75 wt% Fe particles in the Hg fluid.

3. Results

Figure 1 shows line shapes produced by the DSC. The ordinate is proportional to dQ/dt, the heat input to the sample per second, whilst the temperature of the reference sample is increased at a constant scan rate, dT/dt, typically 0.5 or 3.0 K min^{-1}. The total area under the DSC line shape, shown shaded in figure 1(*a*), is a measure of the latent heat of melting whilst the vertical distance between the line shape and base line denoted by $\beta\beta'$ is proportional to the specific heat of the sample. Because of the finite thermal conductivity of the samples and DSC sample holders, a temperature difference exists between the metallic fluid and the reference sample. Consequently a broadening of the line shape occurs as typified by those of figure 1. The rate of heat flow dQ/dt between the sample and sample holder may be considered to be limited by a thermal resistance K defined such that

$$K\,dQ/dt = T_p - T_s \tag{2}$$

where T_s and T_p are the sample and reference sample temperatures respectively. It

follows from equation (2) that as

$$K\,\mathrm{d}^2Q/\mathrm{d}t^2 = (\mathrm{d}T_\mathrm{p}/\mathrm{d}t) - (\mathrm{d}T_\mathrm{s}/\mathrm{d}t) \tag{3}$$

then the gradient of the leading melting edges of the line shape is given by $(\mathrm{d}T_\mathrm{p}/\mathrm{d}t)/K$. This then defines the gradient at which the ordinate is inclined to the abscissae. This must be determined experimentally and is dependent upon the temperature scan rate. Thus, as indicated in figure 1(*a*), the correct melting temperature is given by the intersection of the extrapolated leading edge of the line shape and the base line at the point A. When premelting is observed, as for example in figure 1(*b*), then the leading melting edge of the DSC line shape does not rise sharply from the base line $\beta\beta'$. The magnitude of the premelting is determined from the area BCD. In a similar manner the magnitude of the post-melting, observed in figure 1(*c*), is determined from the area EFG.

Figure 1(*a*) shows the line shape observed during melting for a 0.133 g sample of 99.999% pure triply distilled mercury. No premelting is observed, that is, the extrapolated leading melting edge of the DSC line shape rises sharply from the base line defining a single melting temperature, 234.3 K. Such behaviour is consistent with the high purity of the mercury sample.

Figure 1(*b*) shows the line shape for a mercury based fluid containing 0.75 wt% 4.5 nm diameter iron particles. Premelting is evident, even 10 to 20 deg below the pure mercury melting point. Premelting has the effect of broadening the line shape and consequently reducing the peak height. The area of the premelting region, i.e. the area BCD in figure 1(*b*), is found to be related to the concentration of the iron particles in the mercury.

Figure 1(*d*) shows the observed line shape for a fluid containing sufficient tin to form a monolayer coating on the iron particles. The concentration of the particles in this fluid sample is identical to that of figure 1(*b*). The small inflection in the premelting region is characteristic of all tin–iron–mercury fluids and is more pronounced for viscous concentrated fluids.

In marked contrast to the traces of figures 1(*b*) and (*d*) is the line shape of figure 1(*c*). This is for a 0.4 wt% tin–mercury alloy. This tin concentration is identical to that present in the iron–tin–mercury fluid of figure 1(*d*). For the tin–mercury alloys, structure appears to the right of the melting point and is a consequence of the occurrence of tin–mercury intermetallic phases. This is demonstrated more clearly by comparing the line shapes of the mercury–tin alloys shown in figure 2, which were obtained with a temperature scan rate of 0.5 K min^{-1}, with a simplified portion of the mercury–tin phase diagram (Hansen 1965) shown in figure 3. The structure observed to the right of these line shapes progressively moves to higher temperatures as the tin concentration is increased. That this is to be expected is seen by comparison of the line XY with X′Y′ in figure 3. The same sample was used in figures 1(*c*) and 2(*c*), the line shape differing only because of the differing temperature scan rates of the DSC. From figure 2 it is clearly seen that even as little as 0.5 wt% tin in mercury caused a significant change in the DSC line shape when compared to the line shape of pure mercury shown in figure 1(*a*). As the characteristic line shape structures of tin–mercury alloys are never observed in tin–iron–mercury fluids, it must be concluded that tin–mercury alloys do not form in the presence of iron particles. Thus the tin in iron–mercury fluids is not present in solution but coats the iron particles. This important conclusion is consistent with the magnetic concentration experiments of Hoon (1980), who found that the

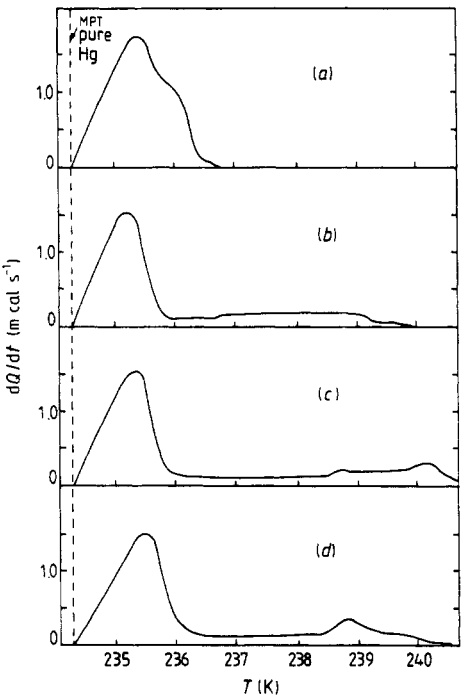

Figure 2. The DSC line shapes for samples of Sn–Hg alloys at scan rates of 0.5 K min^{-1}. (*a*) 0.05 wt%Sn, (*b*) 0.2 wt%Sn, (*c*) 0.4 wt%Sn, (*d*) 0.6 wt%Sn. MPT (234.3 K) pure Hg is denoted by a broken line.

non-magnetic mercury fraction contained no tin as determined from resistivity measurements.

Figure 4 shows both the total latent heat of melting Q_T for tin–mercury alloys as a function of tin concentration and also Q_T for iron–mercury and iron–tin–mercury fluids as a function of iron concentration. The iron–tin–mercury fluids have a tin to iron concentration ratio of 0.54. The tin–mercury alloys exhibit larger latent heats. In contrast, the tin coated and uncoated iron–mercury fluids show a decreasing trend in Q_T with increasing iron particle concentration. The relative error in determining Q_T

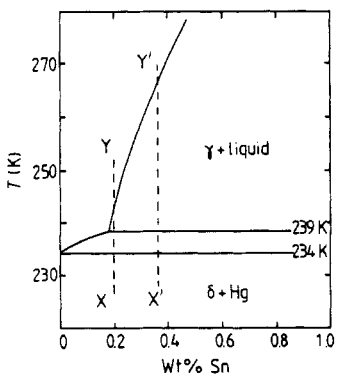

Figure 3. A simplified portion of the mercury rich Sn–Hg phase diagram.

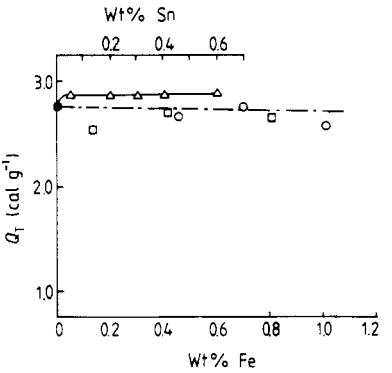

Figure 4. Total heats of transition for various fluids and alloys as a function of Sn and Fe concentration: full circle, pure Hg; open triangle, Sn–Hg; open circle, Sn + Fe particles in Hg, Sn–Fe concentration ratio of 0.54; open square, Fe particles in Hg. The chain line indicates the expected decrease in Q_T due to the absorption of two monolayers of Hg on 4.5 nm diameter Fe particles. The error in each data point is equivalent to the symbol size although systematic errors may be much larger, see text.

from the DSC line shape is $\pm 2\%$, i.e. equivalent to the symbol dimensions in figure 4. However significant random and systematic errors may for instance occur when determining the enthalpy changes for broadened melting reactions such as those of figure 2, where differences in specific heat between solid and liquid phases can lead to uncertainties in the base line. Thus no significance is placed upon the scatter of the points for the iron particles in mercury–tin and in mercury. However in the case of tin–mercury alloys, it is possible that the apparent linearity of Q_T is not entirely fortuitous as this system behaves as a simple, well-defined binary alloy. A plausible explanation for the decreasing trend in Q_T in the case of fluids containing iron particles could be that mercury forms a surface coating on the particles. It would then be possible to consider such a layer as no longer in the liquid phase above the melting point of mercury. In this case it would make a negligible contribution to the latent heat of melting of the fluid. Thus the value of Q_T for the fluid would fall as the iron particle concentration increased. The expected decrease in Q_T may be determined by calculating the mass of mercury needed to form a monolayer coating on the particles. This mass is given by equation (1) if the appropriate parameters for mercury are substituted for those of tin. On this basis, the presence of 1 wt% 3 nm diameter iron particles in mercury would result in a 1% decrease in Q_T per monolayer of absorbed mercury. A similar decrease in Q_T would also result from the absorption of two monolayers of mercury onto 4.5 nm diameter particles. The experimentally observed variation of Q_T in figure 4 would then be consistent with the absorption of between one and two monolayers of mercury on both iron particles and tin-coated iron particles. These calculated changes in Q_T per monolayer are estimates assuming a single particle size. No account has been taken of particle size distributions which are known from electron microscopy and magnetic measurements to exist in all fluids.

4. Contributions to premelting and post-melting

In general 'premelting' is indicative of the presence of solute impurities in the solid state, whilst 'post-melting' is more usually associated with the occurrence of a second

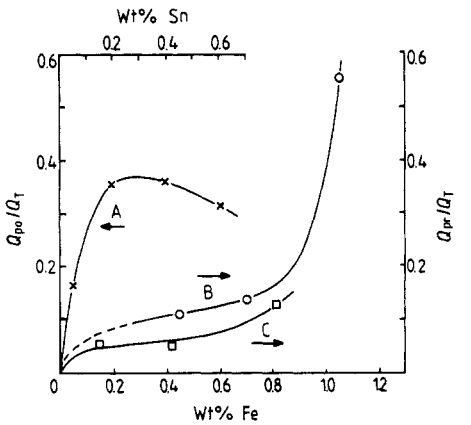

Figure 5. Curve A: ratio of Q_{po}/Q_T for Sn–Hg alloys. Curve B: Ratio of Q_{pr}/Q_T for Sn-coated Fe particles in Hg, Sn–Fe concentration ratio of 0.54. Curve C: Ratio of Q_{pr}/Q_T for Fe particles in Hg.

phase (Ubelohde 1965), as in the case of mercury–tin alloys. Figure 5 shows the fractional contribution that premelting Q_{pr}/Q_T and post-melting Q_{po}/Q_T make to the latent heat of iron–mercury fluids and tin–mercury alloys respectively. The quantity Q_{pr} is defined by the area to the left of the extrapolated bulk melting edge, the latter identified by the broken line in figures 1(*b*) and (*d*). From figure 5 it is seen that for the tin-coated fluid Q_{pr}/Q_T increases sharply for the 1.05 wt% iron fluid. A similar increase in both the viscosity and resistivity with increasing iron concentration has been observed by Hoon *et al* (1978, 1979) and Hoon (1980). Note that there is no similar rapid variation in Q_T with particle concentration. The rapid increase in fluid viscosity at around 1.0 wt% Fe is attributed to the presence and interaction of particle aggregates (Popplewell *et al* 1980, Dixon *et al* 1981). This suggests that the change in Q_{pr}/Q_T which occurs at about 1 wt% Fe may similarly be related to particle aggregation. Further as Q_T is not critically dependent upon iron particle concentration, then it follows that particle aggregation and Q_{pr} must be interrelated.

Also shown in figure 5, by way of contrast, is the very different behaviour of Q_{po}/Q_T for the mercury–tin alloys. These show post-melting (Q_{po}) alone. The different behaviour of Sn–Hg and Sn–Fe–Hg fluids is attributed to the absence of free tin in the latter, due to the presence of the iron particles.

It is possible to analyse the premelting behaviour of Fe–Hg and Fe–Sn–Hg fluids by treating the particles as thermodynamic impurities. Their concentration should then determine the premelting behaviour of the fluid, in accordance with the Raoult–van't Hoff equation (Partington 1952). If F represents the fraction of the sample which has melted at a temperature T_s and T_0 and T_m are the melting points of the pure and impure material respectively then

$$T_s = T_0 - (T_0 - T_m)/F \tag{4a}$$

and

$$(T_0 - T_m) = RT_0^2 x/Q \tag{4b}$$

where R is the gas constant, Q the molar heat of fusion of the pure (mercury carrier) material and x the impurity molarity. Thus F^{-1} versus T_s, plotted for Fe–Hg fluids in

figure 6, should be linear yielding x. The value of F as a function of temperature T is determined by measuring the cumulative area on the low-temperature side of isothermal lines drawn on the DSC line shape, taking care to take account of enthalpy changes that appear as contributions to the apparent specific heat. This method of determining F assumes a linear relationship between the heat effect and the premelting fraction F. This is a reasonable assumption for $F^{-1} \longrightarrow 1$ and thus this region is chosen when estimating the impurity molarity x. Thus from the linear portion of the curves in figure 6, $F > 5\%$, equation (4) implies impurity molarities of 7.8×10^{-4}, 4.3×10^{-4} and 0.4×10^{-4} for the three fluids containing 0.81, 0.41 and 0.14 wt% iron respectively. Defining the impurity molarity as the ratio of the number of iron particles to the number of mercury atoms per unit volume, implies that 4.5 nm diameter iron particles present in the concentrations given above correspond to impurity molarities of 7.1×10^{-4}, 3.6×10^{-4} and 1.3×10^{-4}, respectively. These figures are in fair agreement with the values of x determined from the premelting data. However the van't Hoff equation alone is an inadequate description of Fe–Sn–Hg fluids where inflections are observed in the premelting curves. This suggests that other mechanisms, most probably related to particle aggregation, contribute to the premelting. For example iron particle aggregates are known to include open structures, and thus it is possible that small volumes of mercury may become entrapped within them. As the melting point of finely divided material or small particles is lowered in inverse proportion to their dimensions (as described by Couchman and Ryan (1978) or by Thompson's equation, see Ubelohde (1965)), it is not unreasonable to suppose that some of the entrapped mercury might melt below T_0 in a manner similar to that of a small particle. This or any similar mechanism could be expected to augment the impurity premelting of iron particles in mercury fluids.

5. Concluding remarks

The DSC has provided a direct and novel method of determining the spatial location of tin in tin–iron–mercury magnetic fluids. By comparison of this thermal data to

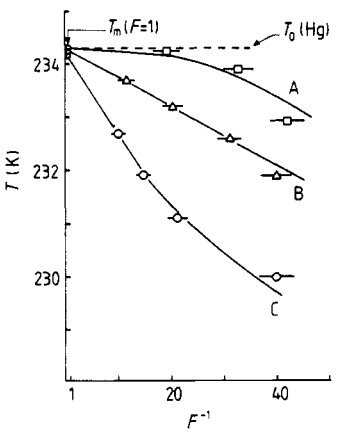

Figure 6. The relationship between fluid temperature (T) and melted volume fraction (F) observed for Fe particles in Hg fluids of concentrations 0.14 wt% Fe (curve A), 0.41 wt% Fe (curve B) and 0.81 wt% Fe (curve C).

previously reported electrical resistivity and viscosity data it is believed that the detail of the solid–liquid transition is dependent not only upon particle concentration but also upon the presence of particle aggregates in the fluid.

Acknowledgments

The support given by the Science Research Council and the US Army, Grant No DAERO-77-G-037 for this work is gratefully acknowledged.

References

Bailar J C 1973 *Comprehensive Inorganic Chemistry* vol 3 (Oxford: Pergamon) pp 275–8
Bennett A J and Duke C B 1967a *Phys. Rev.* **160** 541–53
——1967b *Phys. Rev.* **162** 578–88
Charles S W and Popplewell J 1978 *Thermomechanics of Magnetic Fluids* ed B Berkovsky (Washington DC: Hemisphere) pp 27–44
——1980 *Ferromagnetic Materials* ed E P Wohlfarth (Amsterdam: North-Holland) pp 509–60
Couchman P R and Ryan C L 1978 *Phil. Mag.* A **37** 369–73
Dixon T S, Charles S W and Popplewell J 1981 *J. Phys. F: Met. Phys.* **11** 1931–41
Falk R B and Luborsky F E 1965 *Trans. AIME* **233** 2079–83
Greenwood G W 1956 *Acta Metal.* **4** 243–7
Hansen M 1965 *Constitution of Binary Alloys* (New York: McGraw Hill) pp 837–9
Hoon S R 1980 *PhD Thesis* University of Wales
Hoon S R, Popplewell J and Charles S W 1978 *IEEE Trans. Mag.* **14** 981–3
——1979 *J. Appl. Phys.* **50** 7798–800
Luborsky F E 1957 *J. Phys. Chem.* **61** 1336–40
——1962a *J. Appl. Phys.* **33** 1908–13
——1962b *J. Appl. Phys.* **33** 2385–90
Partington J R 1952 *An Advanced Treatise on Physical Chemistry* vol 3 (London: Longmans) pp 504–11
Popplewell J, Charles S W and Hoon S R 1976 *IEE Conf. Publ. No* 142 pp 13–6
——1980 *IEEE Trans. Mag.* **16** 191–6
Rosensweig R E, Nestor J W and Timmins R S 1965 *Am. Inst. Chem. Eng. Symp. Series* 5 pp 104–18
Ubelohde A R 1965 *Melting and Crystal Structure* (Oxford: Clarendon) pp 5–42, 170–93
Windle P L, Popplewell J and Charles S W 1975 *IEEE Trans. Mag.* **11** 1367–9